

Advancing host-directed therapy for Mycobacterium avium infection: identification of drug candidates and potential host targets

Kilinc, G.

Citation

Kilinc, G. (2025, November 6). *Advancing host-directed therapy for Mycobacterium avium infection: identification of drug candidates and potential host targets*. Retrieved from https://hdl.handle.net/1887/4282119

Version: Publisher's Version

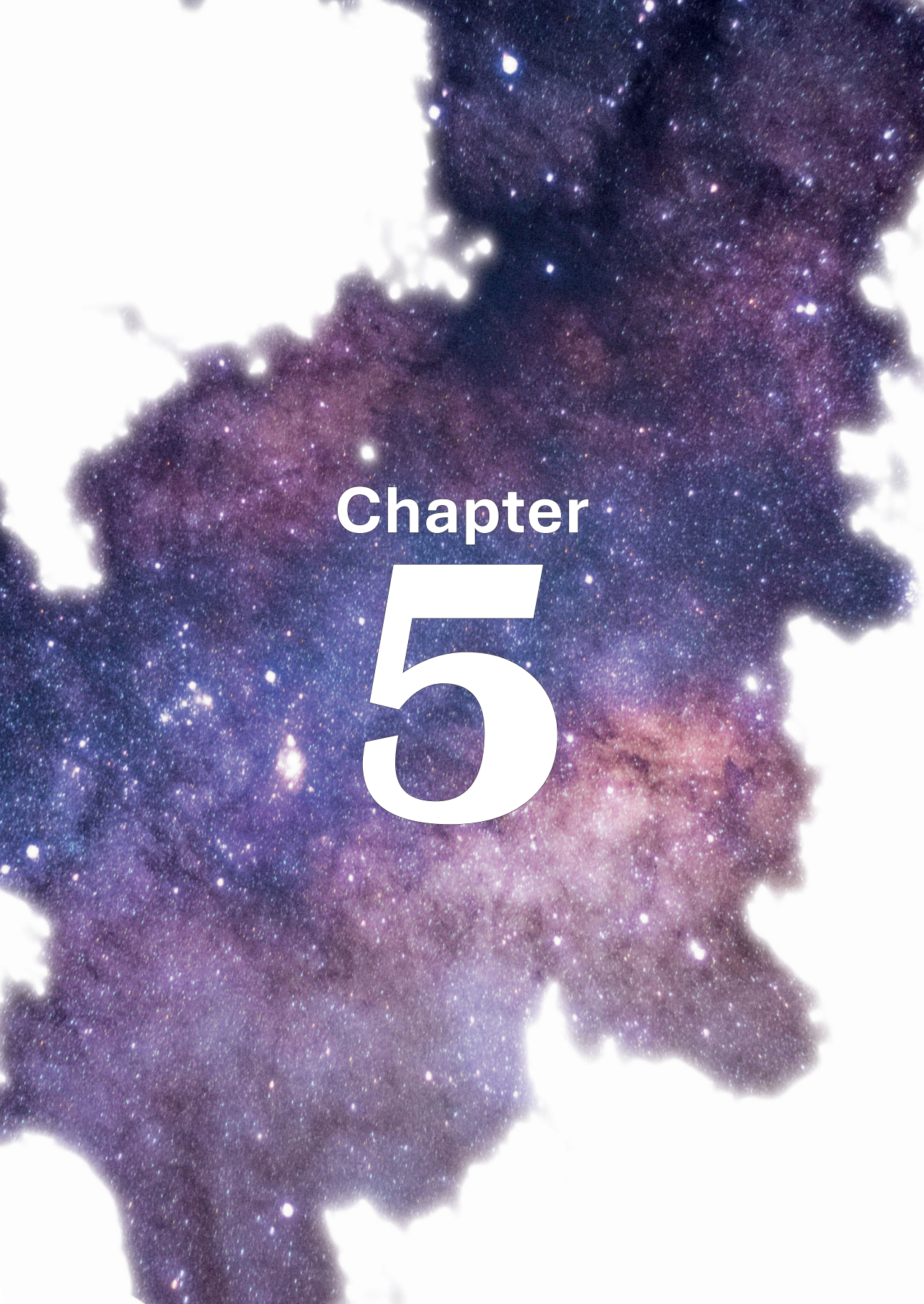
Licence agreement concerning inclusion of doctoral

License: thesis in the Institutional Repository of the University

of Leiden

Downloaded from: https://hdl.handle.net/1887/4282119

Note: To cite this publication please use the final published version (if applicable).



Phenothiazines boost host control of *Mycobacterium avium* infection in primary human macrophages

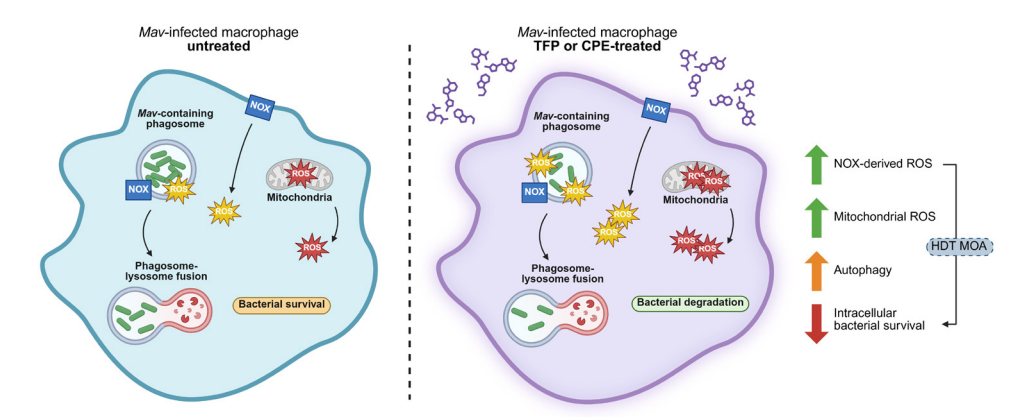
Gül Kilinç¹, Tom H. M. Ottenhoff¹, and Anno Saris¹

¹ Leiden University Center for Infectious Diseases, Leiden University Medical Center, Leiden, The Netherlands

Abstract

Mycobacterium avium (Mav) complex is the leading cause of pulmonary diseases associated with non-tuberculous mycobacterial (NTM) infections worldwide. The inherent and increasing acquired antibiotic resistance of Mav hampers the treatment of Mav infections and emphasizes the urgent need for alternative treatment strategies. A promising approach is host-directed therapy (HDT), which aims to boost the host's immune defenses to combat infections. In this study, we show that phenothiazines, particularly trifluoperazine (TFP) and chlorproethazine (CPE), restricted Mav survival in primary human macrophages. Notably, TFP and CPE did not directly inhibit mycobacterial growth at used concentrations, confirming these drugs function through host-dependent mechanisms. TFP and CPE induced a mild, albeit not statistically significant, increase in autophagic flux along with the nuclear intensity of transcription factor EB (TFEB), the master transcriptional regulator of autophagy. Inhibition of autophagic flux with bafilomycin, however, did not impair the improved host infection control by TFP and CPE, suggesting that the host (auto) phagolysosomal pathway is not causally involved in the mechanism of action of TFP and CPE. Additionally, TFP and CPE increased the production of both cellular and mitochondrial reactive oxygen species (ROS). Scavenging mitochondrial ROS did not impact, whereas inhibition of NADPH oxidase (NOX)-mediated ROS production partially impaired the HDT activity of TFP and CPE, indicating that oxidative burst may play a limited role in the improved host control of Mav infection by these drugs. Overall, our study demonstrates that phenothiazines are promising HDT candidates that enhance the antimicrobial response of macrophages against May, through mechanism(s) that were partially elucidated.

Graphical abstract



- TFP enhances host-directed control of Mav and Mtb in macrophages.
- TFP and CPE enhance macrophage control of Mav independently of autophagy.
- TFP and CPE strongly induce both NOX-derived and mitochondrial ROS production.
- NOX-derived ROS partially aids intracellular Mav infection control by TFP and CPE
- Phenothiazines are promising candidates for HDT against *Mav* infections.

1. Introduction

Nontuberculous mycobacteria (NTM), which comprise all mycobacterial species other than *Mycobacterium tuberculosis* (*Mtb*) and *Mycobacterium leprae*, are environmental microorganisms that have been isolated worldwide. The prevalence of diseases caused by NTM infections is increasing, exceeding that of tuberculosis (TB) in certain geographical regions (1-4). NTM most commonly cause lung disease, but can also lead to lymphadenitis, skin and soft tissue infections, and invasive disseminated disease (5). The *Mycobacterium avium* (*Mav*) complex is the most frequently causative pathogen of NTM infections in humans. Moreover, *Mav* is responsible for the majority of the chronic lung disease cases associated with NTM (6-8). Lung disease by *Mav* (*Mav*-LD) primarily occurs in individuals with predisposing (genetic) lung disorders (e.g. cystic fibrosis or chronic obstructive pulmonary disease) (9, 10), but *Mav*-LD also occurs in those without any known predisposing conditions (11).

The treatment of Mav-LD consists of a three-drug regimen comprising a macrolide, ethambutol, and a rifamycin that should be administered for at least 12 months after negative sputum conversion (5, 12). Despite this, the estimated pooled treatment success rate is only around 40% (13, 14). Furthermore, prolonged treatment duration with multiple drugs could cause adverse effects which hamper treatment adherence, contributing to the suboptimal treatment outcomes for Mav-LD (15). In addition, the resistance of mycobacteria to antibiotics, either intrinsic by their impermeable cell wall and localization in biofilms or cells or acquired due to suboptimal treatment further hampers successful treatment (16). Therefore, there is a pressing need for innovative approaches that improve the therapeutic response and shorten treatment duration, since this will reduce the probability of de novo drug resistance.

Innate immunity plays a critical role in the activation of the host response to mycobacterial infection. Upon inhalation, aerosols containing Mav reach the lower airways where alveolar macrophages provide the first line of defense (17, 18). Recognition of Mav by macrophage pattern recognition receptors, including Toll-like receptors (TLRs) and C-type lectins receptors, induces phagocytosis. Following phagocytosis, the early-forming Mav-containing phagosomes mature and fuse with lysosomes containing hydrolytic enzymes to form phagolysosomes capable of eliminating the mycobacteria (19, 20). In addition, TLR activation induces the production of bactericidal reactive oxygen species (ROS) (21, 22). However, mycobacteria are notorious for their capacity to impair host defense mechanisms, enabling them to persist in macrophages. For example, Mav protein MAV_2941 inhibits phagosome maturation, which thus prevents intracellular Mav killing (23, 24). In addition, predisposing host susceptibility factors, including inherited or acquired defects in the production and signaling of interleukin-12/interleukin-23/interferon-y cascade (25), affect macrophage function, leading to an increased susceptibility to May-LD. Enhancing the antimycobacterial response of macrophages by host-directed therapy (HDT) may therefore improve the clinical outcome of May infection and is a promising adjunctive therapy to antibiotic therapy. By targeting host immunity, HDT may also help to eliminate non-replicating and drug-resistant bacteria that are tolerant or resistant to antibiotic therapy. In addition, adjunctive HDT confers the potential advantages of shortening the duration of current treatment regimens, which may reduce adverse drug effects, and reducing the likelihood of inducing mycobacterial drug resistance since host rather than bacterial pathways are targeted. Although the development of HDT is an active area of investigation in the context of TB, this is largely lacking for *Mav* infections, and it remains unknown whether TB-directed HDT acts also on *Mav* infections.

An approach that has proved to be effective in relatively rapid identification of novel therapeutics against *Mtb* and other bacterial pathogens is drug repurposing (26, 27). Previous screening efforts with different FDA-approved drug libraries have identified several potential HDTs which could restrict intracellular mycobacterial growth (28, 29). A first step towards the identification of HDT candidates for *Mav* may be to employ the findings of the broad screening efforts for *Mtb*. Previously reported screenings of drugs on *Mtb*-infected human cells showed efficacy for several compounds annotated as autophagy-modulators, including trifluoperazine (TFP), in improving host control of infection (29). In this study, we aimed to assess the potential of TFP and related compounds as HDT against *Mav* and unravel the underlying host immune responses involved.

We identified phenothiazines as potential HDT candidates to control *Mav* bacteria in primary human macrophages. Importantly, these compounds did not show a direct antibacterial effect at the concentration in which they enhanced clearance of intracellular *Mav*, showing that phenothiazines must act via host signaling pathways. To unravel the mechanism of action, we investigated potential host antimicrobial mechanisms that have been associated with TFP.

2. Results

2.1 In vitro identification of phenothiazines as potential HDT for Mav infection

Based on previous screening efforts to identify new drugs with HDT activity against intracellular Mtb, trifluoperazine (TFP) was identified as a promising candidate (29). Before evaluating its potential to enhance clearance of intracellular Mav infection, the antimycobacterial effect of TFP on Mtb was first validated in a more physiologically relevant model. Screening of TFP decreased survival of Mtb in two polarized macrophages subsets, pro-inflammatory M1 and anti-inflammatory M2 macrophages (30), as determined by the MGIT system after treatment of 24 hours with 10 µM of the drug, identifying the phenothiazine-class of antipsychotic drugs as potential HDT candidates (Fig. 1A-B). To identify the most potent phenothiazine drug for Mav, we expanded the screening to include TFP and 15 additional (total 16) structurally related phenothiazines using the primary human macrophage model (31). The results showed a higher activity of phenothiazines in M1 compared to M2 macrophages (Fig. 1C). Five compounds showed significant impairment of bacterial survival in M1 macrophages: trifluoperazine (TFP), chlorproethazine (CPE), ZINC2187528 (ZINC), fluphenazine (FPZ) and chlorprothixene (CPT) (Fig. 1C-D). This effect was dose-dependent, as the drugs rapidly lost their ability to significantly impair intracellular bacteria at concentrations below 1 µM (Supp Fig. 1). In M2 macrophages, only CPE was able to significantly reduce the bacterial load (Fig. 1C and 1E). Importantly, treatment with TFP, CPE, ZINC, FPZ, and CPT did not affect the cell viability of Mav-infected M1 or M2 macrophages (Fig. 1F-G).

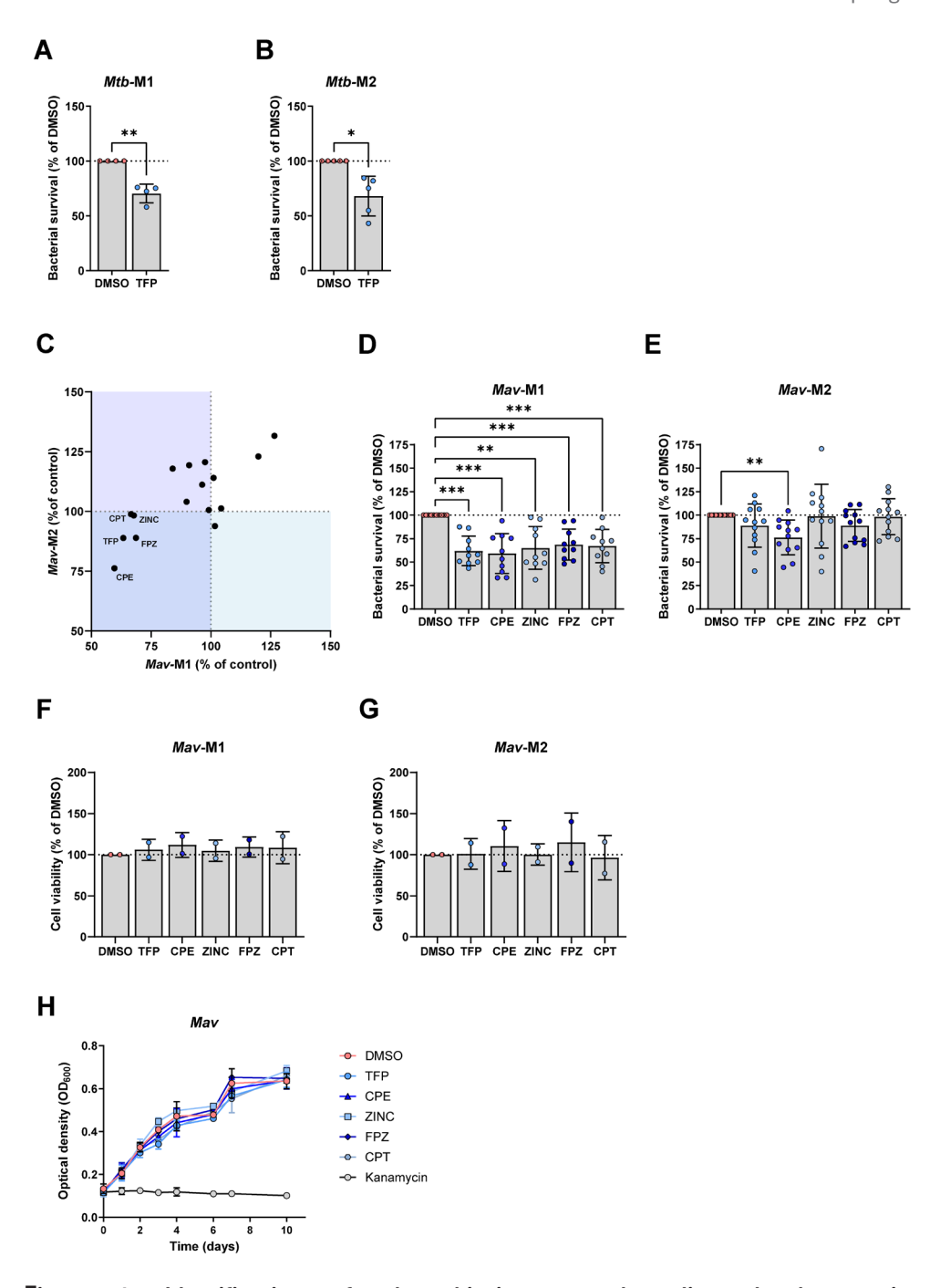


Figure 1. Identification of phenothiazines as host-directed therapeutics against Mav and Mtb in primary human macrophages. (A-B) Bacterial survival of Mtb within M1 and M2 macrophages after treatment with $10\,\mu\text{M}$ TFP or DMSO for 24 hours, as determined by the MGIT assay (n=4 or 5). Statistical significance was tested using a repeated-measures one-way ANOVA with Dunnett's multiple comparisons test. (C) Bacterial survival of Mav within

M1 and M2 macrophages after treatment with 10 μ M of 16 phenothiazines or DMSO for 24 hours, as determined by the MGIT assay (n=4). Dots indicated with name represent compounds that reduced intracellular bacterial survival in either M1 or M2 macrophages. (**D-F**) Bacterial survival of *Mav* within M1 and M2 macrophages after treatment with 10 μ M of the five effective compounds from A or DMSO for 24 hours, as determined by the MGIT assay (n=10 or 12). Statistical significance was tested using a repeated-measures one-way ANOVA with Dunnett's multiple comparisons test. (**F-G**) Percentage of viable *Mav*-infected M1 and M2 macrophages after treatment with 10 μ M of the five effective phenothiazines or DMSO for 24 hours (n=2). (**H**) Growth of *Mav* in liquid broth up to 10 days after exposure to positive control 100 μ g/mL kanamycin, 10 μ M of phenothiazines, or DMSO. Data represent the mean ±SD of triplicate wells from three independent experiments.

Dots represent the mean from triplicate wells of a single donor. Data represent the mean \pm standard deviation (SD) from different donors and is expressed as a percentage of vehicle control DMSO (=100%, indicated with the dotted line) per donor. TFP; trifluoperazine, CPE; chlorproethazine, ZINC; ZINC2187528, FPZ; fluphenazine, CPT; chlorprothixene. *= p<0.05, **= p<0.01 and ***= p<0.001.

To confirm that the TFP analogs reduced bacterial loads in a host-mediated manner, May in liquid medium was exposed to 10 µM of the drugs, the same concentration used as in the above Mav intracellular screenings. The TFP compounds did not affect the growth of Mav, whereas positive control kanamycin inhibited bacterial growth (Fig. 1H). Phenothiazine-derived molecules are cationic amphiphilic drugs (CADs), which have both lipophilic properties (logP > 1), enabling them to passively diffuse across cell and organelle membranes, and a weak base character (pKa > 8) that cause them to become positively charged under acidic conditions (Supp Fig. 2A) (32). These characteristics cause the drugs to become trapped within acidic compartments such as lysosomes, leading to increased intracellular drug concentrations. Therefore, we correlated the supposed ability of the drugs to reduce intracellular bacterial load with their tendency to accumulate intracellularly. After exposure of planktonic bacteria to 100 µM, growth (i.e., extracellular survival) was inhibited by the majority of phenothiazines whereas the ability of the compounds to impair intracellular bacteria, however, strongly varied between structural analogs (Supp Fig. 2B). The discrepancy between intra- and extracellular activity between compounds could not be explained by their tendency to accumulate intracellularly and direct inhibition of bacterial growth at higher concentrations (Fig. 2A-B). Thus, mere accumulation is an unlikely cause of the intracellular activity of phenothiazines, and host-directed mechanisms are more likely at play. Taken together, we identified host-directed therapy with phenothiazines that impaired the survival of intracellular Mav in M1 macrophages, and to a lesser extent in M2 macrophages.

To investigate the mechanism by which phenothiazines eliminated intracellular mycobacteria, we focused on TFP and CPE in M1 macrophages (in which more analogs were effective, **Fig. 1A-B**). The foremost function of phenothiazines is their antagonistic effect on D2 dopamine receptors (33, 34), receptors that are also expressed by macrophages (35). We, therefore, investigated if dopamine receptors were involved in the improved control of *Mav* infection by CPE. The addition of dopamine or quinpirole (D2 receptor agonist) did not affect bacterial survival in *Mav*-infected macrophages treated with CPE (**Supp Fig. 3A-B**). Of note, dopamine agonists in the absence of phenothiazines, in particular quinpirole, enhanced intracellular *Mav* killing,

suggesting that antagonism of dopamine D2 receptors by phenothiazines is unlikely the cause for the enhanced macrophage response to *Mav* infection. Consequently, we examined the contribution of additional intracellular host antibacterial pathways.

2.2 Improved host macrophage antimicrobial response by TFP and CPE is independent of autophagy induction

As described above, TFP and CPE are CADs, which are also known to induce phospholipidosis, a cellular phenotype caused by impaired degradation of phospholipids. To overcome phospholipidosis, cells can upregulate autophagy by enhancing the activation of transcription factor EB (TFEB), a major regulator of autophagy. Recently, CAD amiodarone was shown to impair the intracellular survival of mycobacteria by inducing autophagy via TFEB activation (36). We therefore determined whether TFP and CPE compounds induced the accumulation of phospholipids as well as activation of TFEB in *Mav*-infected macrophages. Macrophages treated with TFP or CPE showed increased accumulation of fluorescent phospholipid phosphatidylethanolamine (NBD-PE) (**Fig. 2A**). In addition, the nuclear intensity of TFEB was increased in macrophages treated with TFP or CPE, albeit not significant (p=0.051 or p=0.178, respectively) (**Fig. 2B-C**), supporting the notion that autophagy might be induced.

To further determine whether the induction of phospholipidosis could be associated with the induction of actual autophagy, the effect of TFP and CPE on autophagy markers during Mav infection was assessed by western blot (Fig. 2D). The levels of autophagosome component LC3-II were measured in the presence or absence of the (auto-)lysosomal inhibitor bafilomycin A1 (Baf); LC3-II levels indicate the formation of autophagosomes and the extent of LC3-II accumulation in presence of bafilomycin corresponds to autophagic flux. Both TFP and CPE treatment tended to increase protein levels of LC3-II, both in the absence and presence of bafilomycin (Fig. 2E). The autophagy response to intracellular pathogens can occur as a receptor-mediated process (selective autophagy or xenophagy) or more generally as a stress response (non-selective autophagy). To discriminate between these forms of autophagy, we examined p62, which selectively recruits polyubiquitinated cytoplasmic substrates to autophagosomes where p62 and the substrates are degraded (37, 38). Levels of p62 tended to be decreased in macrophages treated with TFP, while p62 flux remained unaffected by CPE (Fig. 2F). Furthermore, levels of lysosomal marker LAMP1 were not affected upon treatment with TFP and CPE (Fig. 2G). To determine whether the autophagy pathway was causally involved in the elimination of intracellular Mav, HDT activity of TFP and CPE was evaluated in Mav-infected macrophages whilst autophagymediated degradation was blocked using bafilomycin. Treatment with TFP and CPE reduced bacterial survival irrespective of inhibition of autophagy with bafilomycin (Fig. 2H). Collectively, these results show that while autophagy is affected by TFP and CPE treatment, the enhanced macrophage antimicrobial response upon treatment is independent of the induction of autophagy.

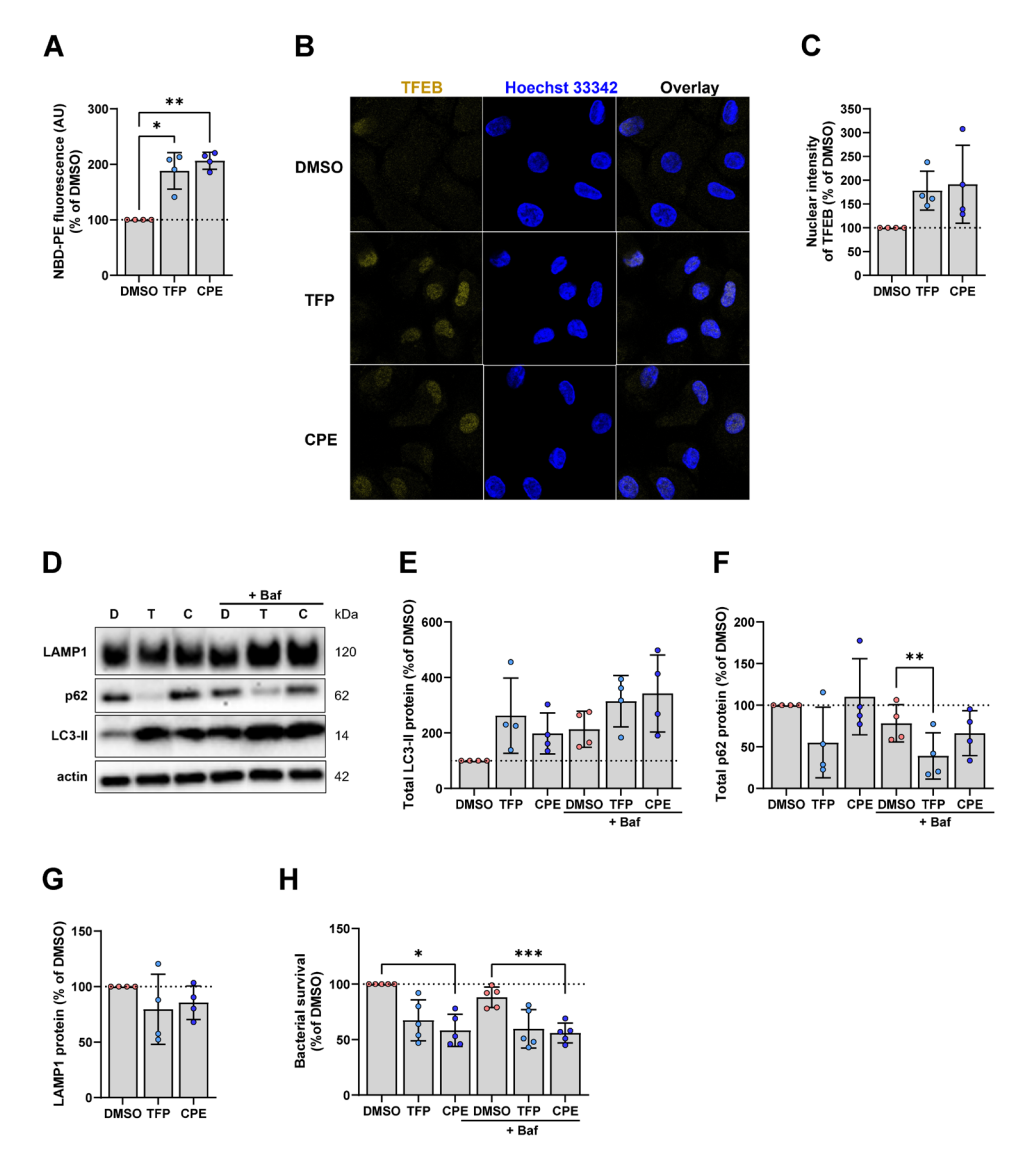


Figure 2. TFP and CPE do not require the host autophagy pathway to control Mav infection in primary human macrophages. (A) Mav-infected M1 macrophages were treated with $10\,\mu\text{M}$ TFP, CPE, or DMSO and $5\,\mu\text{M}$ NBD-PE for 24 hours to assess phospholipidosis induction (n = 4). Statistical significance was tested using a repeated-measures one-way ANOVA with Dunnett's multiple comparisons test. (B) Confocal microscopy of Mav-infected M1 macrophages treated with $10\,\mu\text{M}$ TFP, CPE, or DMSO for 4 hours, stained for TFEB (yellow) and Hoechst 33342 (blue). Shown are images of one representative donor out of four donors tested. (C) Quantification of TFEB intensity within the mark of the cell nucleus. Dots represent the mean from three wells (three images/well) per condition of a single donor (n = 4). Statistical significance was tested using a repeated-measures one-way ANOVA with Dunnett's multiple comparisons test. (D-G) Western blot analysis of autophagy markers in M1 macrophages treated with $10\,\mu\text{M}$ TFP, CPE DMSO with or without $10\,n\text{M}$ bafilomycin A1 (Baf) for 4 hours during Mav infection. Shown are blots from one representative donor (D). Quantified protein levels of LC3-II (E), p62 (F), or LAMP1 (G) were normalized to actin (n = 4). Statistical significance was tested using a repeated-

measures one-way ANOVA with Bonferroni's (E-F) or Dunnett's (G) multiple comparisons test. **(H)** Bacterial survival of *Mav* within M1 macrophages treated with TFP, CPE or DMSO with or without 10 nM Baf for 24 hours, as determined by the MGIT assay (n=5). Statistical significance was tested using a repeated-measures one-way ANOVA with Bonferroni's multiple comparisons test. Dots represent the mean from triplicate wells of a single donor. Data represent the mean \pm standard deviation (SD) from different donors and is expressed as a percentage of vehicle control DMSO (=100 %, indicated with the dotted line) per donor. TFP; trifluoperazine, CPE; chlorproethazine. *= p<0.05, **=p<0.01 and ***=p<0.001.

2.3 NOX-derived ROS might play a limited role in TFP and CPE-enhanced host control of *Mav* infection

In addition to the autophagy pathway, the production of reactive oxygen species (ROS) has also been reported to be affected by TFP (39, 40). ROS represents another important host antimicrobial mechanism for the eradication of intracellular bacteria (41), leading us to investigate the role of ROS in the mechanism of action of both TFP and CPE. Two major sources of ROS are NADPH oxidases (NOX), located at the cell- or phagosomal- membrane, and complex I of the respiratory electron transport chain (ETC) of mitochondria (Fig. 3A). Using the fluorescent probe CellROX, total cellular ROS in May-infected macrophages treated with TFP or CPE was measured while the production of ROS by mitochondria was determined using the fluorescent probe MitoSOX. Both TFP and CPE significantly induced total ROS production (Fig. 3B). Also levels of mitochondrial ROS were significantly increased in Mav-infected macrophages after treatment with TFP or CPE (Fig. 3C). Even in the absence of infection, TFP and CPE enhanced both cellular and mitochondrial ROS in macrophages (Supp Fig. 4A-B). To determine whether the induction of (mitochondrial) ROS mediates TFP and CPEenhanced host control of Mav infection, Mav-infected macrophages were treated with TFP or CPE in the presence of a variety of ROS scavengers. Known scavengers of cellular ROS, N-acetyl-cysteine (NAC) and reduced L-glutathione, failed to reduce ROS production during treatment with TFP and CPE and/or posed cell toxicity at concentrations used (Supp Fig. 4C-F) (42). While NAC is commonly depicted as a broad-spectrum ROS scavenger, NAC is unable to scavenge all types of ROS (43-45), and was unable to scavenge the types of ROS induced by TFP and CPE. Also MnTBAP (a superoxide dismutase mimic) did not inhibit cellular ROS production (Supp Fig. 4G) (46). In contrast, VAS2870, a pan-NOX inhibitor (47, 48), partially reduced cellular ROS production in control and induced by TFP and CPE (median percentage ROS induction compared to control reduced from 72% to 17% and from 134% to 72%, respectively) (Fig. 3D). Whilst these differences were not statistically significant, the addition of VAS2870 impaired the ability of TFP and CPE to reduce intracellular survival of Mav (inhibition of bacterial survival decreased from 21% to +12% and from 33% to 4%, respectively, compared to controls) (Fig. 3E). Thus, NOX-mediated ROS production is involved, at least to some extent, in the macrophage response to Mav improved by TFP and CPE.

To assess the role of mitochondrial ROS in the mode of action of TFP and CPE, MitoTEMPO (a mitochondria-targeted scavenger), rotenone (an inhibitor of complex I of the ETC) and MnTBAP were used. MitoTEMPO was ineffective in reducing TFP and CPE-induced mitochondrial ROS production (**Supp Fig. 5A-B**). If mitochondrial ROS

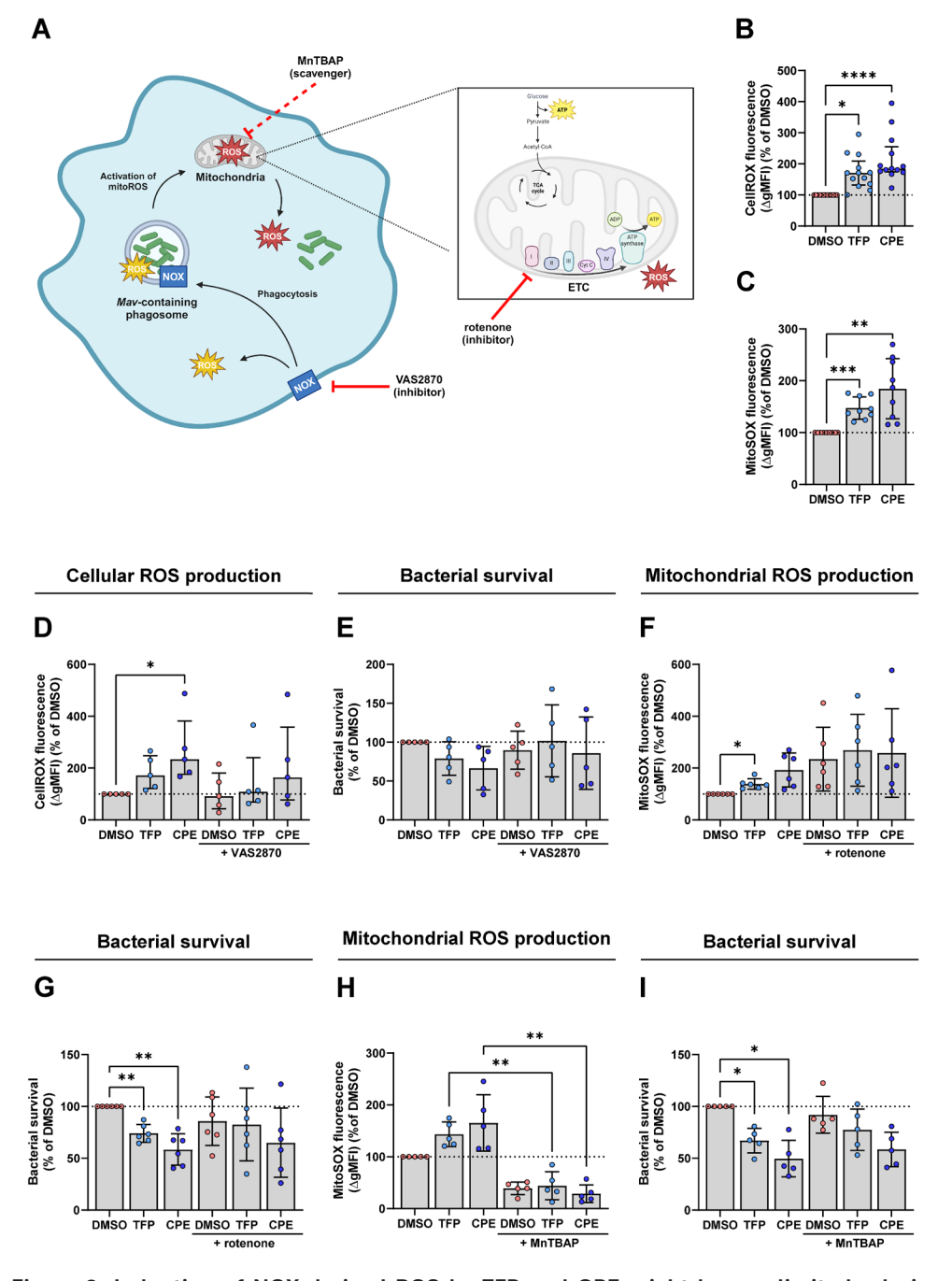


Figure 3. Induction of NOX-derived ROS by TFP and CPE might have a limited role in their enhanced macrophage response against *Mav.* (A) Schematic overview of the two major sources of ROS production in macrophages: NADPH oxidases (NOX) at (phagosomal) membranes and mitochondrial electron transport chain (ETC). Used ROS modulators: VAS2870 (NOX inhibitor), MnTBAP mitochondrial superoxide scavenger (dotted inhibition arrow), and

rotenone (ETC complex I inhibitor). (B-C) Mav-infected M1 macrophages were treated with 10 µM TFP, CPE or DMSO for 4 hours. Total cellular ROS production (B) or mitochondrial ROS (C) production was measured by flow cytometry. The geometric mean fluorescence intensity (ΔgMFI) was determined. Data represent the median ± interquartile range (B, n = 13) or mean ±SD from (C. n=9). Statistical significance was tested using a Friedman test with Dunn's multiple comparisons test (B) or a repeated-measures one-way ANOVA with Dunnett's multiple comparisons test (C). (D-E) M1 macrophages were treated with 10 uM TFP. CPE. or DMSO with or without 10 µM VAS2870 for 4 (D) or 24 (E) hours after Mav infection. Total cellular ROS production was detected by flow cytometry. The geometric mean fluorescence intensity (ΔgMFI) (D) or bacterial survival by CFU assay (E) were determined. Data represent the median ±interquartile (D) or the mean ±SD (E) from different donors (n=5). Statistical significance was tested using a Friedman test with Dunn's multiple comparisons test (D) or a repeated-measures one-way ANOVA with Bonferroni's multiple comparisons test (E). (F-G) M1 macrophages were treated with 10 µM TFP, CPE, or DMSO with or without 5 µM rotenone for 4 (F) or 24 (G) hours after Mav infection. Total mitochondrial ROS production was detected by flow cytometry. The geometric mean fluorescence intensity (AgMFI) (F) or bacterial survival by CFU assay (G) were determined. Data represent the mean ±SD from different donors (n=6). Statistical significance was tested using a repeated-measures one-way ANOVA with Bonferroni's multiple comparisons test. (H-I) M1 macrophages were treated with 10 µM TFP, CPE, or DMSO with or without 100 µM MnTBAP for 4 (H) or 24 (I) hours after Mav infection. Total mitochondrial ROS production was detected by flow cytometry. The geometric mean fluorescence intensity (ΔgMFI) (H) or bacterial survival by CFU assay (I) were determined. Data represent the mean ± SD from different donors (n = 5). Statistical significance was tested using a repeated-measures one-way ANOVA with Bonferroni's multiple comparisons test. Dots represent the mean from duplicate wells of a single donor. Data is expressed as a percentage of vehicle control DMSO (=100 %, indicated with the dotted line) per donor. TFP; trifluoperazine, CPE: chlorproethazine. *= p < 0.05, ** = p < 0.01, *** = p < 0.001 and **** = p < 0.0001.

is produced by complex I of the ETC via the engagement of reverse electron transport (RET), rotenone will decrease ROS production, however if RET does not occur, rotenone will increase ROS production (49, 50). Here, rotenone mildly enhanced the induction of mitochondrial ROS, but did not affect the intracellular control of *Mav* by TFP and CPE (**Fig. 3F-G**). Moreover, MnTBAP significantly reduced levels of mitochondrial ROS induced by TFP or CPE in *Mav*-infected macrophages (mean percentage ROS induction compared to control reduced from 43% to 5% and from 65% to -11%, respectively) (**Fig. 3H**). Despite this substantial reduction in mitochondrial ROS, MnTBAP had a negligible effect on the intracellular control of *Mav* after TFP and CPE treatment (inhibition of bacterial survival decreased from 33% to 14% and from 50% to 33%, respectively, compared to controls) (**Fig. 3I**). Thus, while TFP and CPE induce mitochondrial ROS production, this is not causally involved in the reduced intracellular survival of *Mav*.

To exclude any false positive results caused by direct inhibition of bacterial growth by the ROS modulators, the effects of VAS2870, MnTBAP, and rotenone on bacterial growth were assessed in the absence of macrophages. Neither of the ROS modulators directly inhibited bacterial growth (**Supp Fig. 5C**). Moreover, cell death could also result in decreased intracellular bacterial load and falsely indicate that TFP and CPE act via HDT activity despite ROS modulation. VAS2870, MnTBAP, and rotenone, however, did not induce cell toxicity to *Mav*-infected macrophages (**Supp Fig. 4H and Supp Fig. 5D-E**). Taken together, these findings show that ROS production, particularly from NOX, seems to be involved in the improved host control of intracellular *Mav* induced by TFP and CPE.

3. Discussion

In this study, we identified phenothiazines, a class of antipsychotic drugs, as novel HDT candidates for the elimination of intracellular Mav. TFP, CPE, ZINC, FPZ, and CPT enhanced host control of Mav in primary human M1 macrophages at concentrations that did not directly impair bacterial growth, indicating that intracellular host rather than bacterial processes are modulated that resulted in reduced intracellular survival of Mav. To identify the mechanism of action, we evaluated two well-known host antibacterial pathways that are reported to be affected by TFP: autophagy and ROS production. While TFP and CPE treatments showed a trend toward induction of autophagy, this pathway was not mechanistically involved in the HDT effect of both compounds. In addition, TFP and CPE strongly induced the production of ROS without impairing cell viability. Reducing ROS production in mitochondria had no impact on bacterial survival, while inhibiting ROS from NOX partially restored the survival of intracellular Mav after TFP and CPE treatment. Hence, as reducing (NOX-mediated) ROS production did not fully restore the impaired bacterial survival after TFP and CPE treatment, we hypothesize that other mechanisms yet to be discovered are also at play.

Phenothiazines have been shown to have antimicrobial activity against a wide range of bacteria, including Staphylococcus aureus (51, 52), Mtb and Mav (53-59), by affecting multiple essential bacterial functions. At concentrations that effectively reduced intracellular Mav levels, both TFP and CPE did not have direct antimycobacterial activity, in line with previous observations that showed phenothiazines eradicated intracellular Mtb and Mav by macrophages (55, 60, 61), although the specific host cellular pathways involved were not addressed. Being CADs, which can accumulate intracellularly, the possibility remained that TFP and CPE might accumulate in acidic compartments in macrophages to reach antibacterial concentration levels. However, the ability of different phenothiazines to impair intracellular mycobacterial survival did not correlate with its antibiotic potency related to intracellular drug accumulation, suggesting that mere accumulation is unlikely the cause of the HDT effect and rather host-dependent mechanisms are at play. This finding aligns with previous research that shows that phenothiazine derivatives decrease bacterial burden within the host without directly affecting bacteria themselves, suggesting that these drugs modulate host cell pathways necessary to control infection (62-64).

Activation of the host autophagy pathway has been shown to reduce intracellular *Mav* burden (65), yet *Mav* has also evolved strategies to counteract this by interfering with phagosome-lysosome fusion to survive intracellularly (66, 67). Depending on the cell lines and drug concentrations used, phenothiazines have been shown to either suppress or induce autophagy (68). Suppression of autophagy may be the result of calmodulin inhibition by phenothiazines (69-71). Calmodulin is a cytosolic binding protein that is recruited and activated following increased cytosolic calcium levels in macrophages encountering mycobacteria (72, 73). The Ca²⁺-Calmodulin complex promotes the maturation of phagosomes required for autophagy (73). In contrast, TFP is also described to promote autophagic flux in cells, including lung cell lines, and zebrafish (71, 74). Other phenothiazines than TFP promoted acidification of the phagolysosome, thereby improving intracellular killing of mycobacteria (61, 75). Previously, TFP was shown to induce autophagy in HeLa cells infected with *Salmonella*

Typhimurium and to improve clearance of intracellular infection, although it remains unclear whether these effects are causally linked (76). In the current study, TFP and CPE mildly enhanced autophagic flux and a noticeable trend in TFEB activation, in line with previous observations (77). Nevertheless, blocking autophagy and acidification did not impair the antimycobacterial HDT effect of TFP and CPE on intracellular bacteria, which indicates that lysosomal degradation is likely not essential for the host-protective effect of phenothiazines.

Another host pathway that is known to be fundamental for macrophages to kill invasive pathogens is ROS production (78). TFP has been shown to increase both cellular and mitochondrial ROS levels in our as well as other studies (39, 79). Two major sources of ROS are NADPH oxidases (NOX) and the mitochondrial electron transport chain (ETC) (41). NOX enzymes, primarily located on the plasma membrane, produce cytosolic ROS. During phagocytosis, the plasma membrane forms the interior wall of the phagocytic vesicle, releasing ROS into the vesicle to kill pathogens (78). ROS production induced by TFP and CPE was in part derived from NOX, as NOX inhibition only partially impaired ROS production. NOX-inhibition also restored bacterial survival after TFP and CPE treatment to a certain extent, suggesting that NOX plays a role in eliminating intracellular Mav by TFP and CPE. Furthermore, mitochondrial ROS, traditionally seen as a by-product of respiration and indicative of oxidative stress (41), is now also recognized as an important antibacterial response in innate immune cells (78, 80). In addition, mitochondrial ROS production via RET from complex II to complex I of the ETC was shown to promote intracellular killing of Mav (81). Our finding that TFP and CPE induced mitochondrial ROS production seemingly without involvement of RET, therefore, may explain why mitochondrial ROS is not involved in enhanced macrophage response induced by TFP and CPE against intracellular Mav. The discrepancy in the occurrence of RET within Mav-infected macrophages between this and the study by Røst et al. might be attributed to variations in the experimental setup (81), including the longer infection and shorter treatment duration until the readout of ROS in our study. Taken together, these findings suggest that while both NOX-mediated and mitochondrial ETC-mediated ROS production are induced, only the ROS production driven by NOX to a limited extent can account for the enhanced host control of Mav by TFP and CPE.

Phenothiazines are approved as drugs for the treatment of neurological disorders such as schizophrenia by inhibiting dopamine receptors (82, 83). While dopamine has been extensively studied for its role in the central nervous system, emerging evidence indicates its role as an immunomodulator in innate immunity (35). Treatment of macrophages with dopamine showed activation of NF-Kb leading to increased secretion of pro-inflammatory cytokines and chemokines (84-86), which are associated with macrophage activation and control of mycobacterial infections (87-89). Similarly, we show that dopamine receptor agonists improved control of intracellular *Mav* infection regardless of the presence of phenothiazines. Therefore, TFP and CPE, being dopamine receptor antagonists, reduce intracellular *Mav* loads likely by a mechanism independent of dopamine receptor antagonism. Moreover, TFP inhibits dopamine receptors at nanomolar concentrations (90), yet its host-directed effects against *Mav* were only evident at micromolar concentrations. The notion that TFP and CPE control *Mav* infection independent of dopamine receptors is supported

by the finding that structural modifications abolishing dopamine receptor binding did not affect phenothiazines' ability to inhibit intracellular *Mtb* growth (91). Hence, eliminating the dopamine receptor-dependent psychotropic effects of phenothiazines while maintaining their HDT activity against intracellular bacteria seems feasible.

Limitations of our study may be that, although HDT would likely be used as adjunctive therapy in clinical settings, the efficacy of phenothiazines in combination with conventional antibiotics was not assessed, as the primary focus was to discover the mechanism of action of phenothiazines. Future studies should explore drug interactions and effects on the efficacy of phenothiazines when combined with antibiotics, to design shorter, more effective, and safer drug regimens. In addition, when deciphering the mechanisms of phenothiazines, the focus was on M1 macrophages without examining the mechanistic effects on M2 macrophages. M1 macrophages are critical for immediate pathogen clearance, whereas M2 macrophages may involve different cellular pathways potentially linked to drug efficacy. Furthermore, while we investigated major sources of ROS production, the role of other ROS sources such as peroxisomes or cytochrome P450 enzymes was not explored (41). Although limited information exists on how these sources impact macrophage-mediated immunity, these minor ROS sources could play a role in the HDT activity of TFP and CPE which warrants further research. Moreover, although we suggest that TFP and CPE likely act independently of dopamine receptors, we cannot rule out receptor involvement entirely. Irrespectively, as these compounds are known to interact with dopamine receptors, concerns about (e.g., cognitive) side effects could limit their use for treating mycobacterial infections. Additionally, the effective concentration of TFP (and CPE) in our study exceeds the peak plasma levels (1.3-7.6 nM) following oral administration of a 5 mg TFP tablet (initial twice-daily dosing for the treatment of schizophrenia) (92). Ideally, phenothiazines will be chemically modified to reduce their binding to dopamine receptors while enhancing their antimycobacterial activity, which may improve the therapeutic window during clinical application. Another approach to address this issue may be alternative drug delivery strategies such as nanoencapsulation of TFP and CPE (93), which may limit systemic exposure and reduce toxicity risks while enabling localized drug delivery to infected macrophages. While we aimed to identify the mechanism of action, phenothiazines may improve host control of intracellular May by acting on multiple pathways. The pleiotropy of phenothiazines makes it extremely challenging to detect significant effects when only one pathway is analyzed at a time. Although the exact mechanisms of action of phenothiazines remain unidentified, our study rules out host autophagy and suggests that cellular ROS production plays a moderate role, thereby guiding the focus for future research. Given that Mav exploits various antioxidative strategies to evade host defenses (94-97), investigating by which mechanisms phenothiazines induce (NOX-derived) ROS production could provide valuable insights into how these bacterial defenses can be counteracted and how these drugs enhance macrophage activity against mycobacteria. By highlighting the potential of phenothiazines as novel HDT candidates, our study may contribute to the development of more effective therapeutic strategies to combat mycobacterial infection.

Our findings show that phenothiazines act via host-dependent mechanisms to promote the clearance of *Mav* within macrophages. Nevertheless, the precise

mechanisms underlying their therapeutic effects were only partially unraveled and require further investigation. Elucidating these mechanisms will not only deepen our understanding of host-pathogen interactions during *Mav* infection but will also facilitate the development of targeted therapeutic strategies utilizing phenothiazine-derived compounds as HDT for intracellular bacterial infections.

4. Materials and methods

4.1 Reagents and antibodies

Anti-human CD163-PE, CD14-PE-Cy7, and CD1a-Alexa Fluor 647 (1:20) were purchased from Biolegend (Amsterdam, the Netherlands), and anti-human CD11b-BB515 (1:20) from BD Biosciences. For confocal microscopy, rabbit anti-human TFEB (1:200) from Cell Signaling Technology (Leiden, the Netherlands), and donkey anti-rabbit IgG (H + L)-Alexa Fluor 555 (1:200) from Abcam (Amsterdam, the Netherlands) were used. Hoechst 33342 (1:2,000) was obtained from Sigma-Aldrich (Zwijndrecht, the Netherlands). For western blot, rabbit anti-human LC3B (1:500) from Novus Biologicals/Bio-Techne (Abingdon, UK), mouse anti-human SQSTM1/p62 (1:500) from Santa Cruz Biotechnology (Heidelberg, Germany), rabbit anti-human LAMP1 (1:500) from Abcam and mouse anti-human β -actin (1:1,000) from Sigma-Aldrich were used. Horseradish peroxidase-conjugated goat anti-rabbit IgG (H + L) and goat anti-mouse IgG (H + L) (1:5,000) were purchased from Invitrogen, ThermoFisher Scientific (Landsmeer, the Netherlands).

N-4-nitrobenzo-2-oxa-1,3-diazole-phosphatidylethanolamine (NBD-PE), CellROX, and MitoSOX probes were purchased from Invitrogen, ThermoFisher Scientific. Trifluoperazine dihydrochloride was obtained from Enzo Life Sciences (Brussels, Belgium), chlorproethazine hydrochloride from Toronto Research Chemical, chlorprothixene from Vitas-M Laboratory (Apeldoorn, the Netherlands), fluphenazine dihydrochloride from Sigma-Aldrich and ZINC218752 from Specs (Zoetermeer, the Netherlands). Dimethyl sulfoxide (DMSO), bafilomycin A1, kanamycin sulfate, dopamine hydrochloride, quinpirole hydrochloride, N-acetyl-L-cysteine, L-glutathione reduced, MitoTEMPO, MnTBAP, VAS2870, and rotenone were purchased from Sigma-Aldrich.

4.2 Cell culture

Buffy coats were collected from healthy anonymous Dutch adult donors who provided written informed consent (Sanquin Blood Bank, Amsterdam, the Netherlands), to isolate primary monocyte-derived macrophages as previously described (45). In summary, CD14+ monocytes were isolated from peripheral blood mononuclear cells using density gradient centrifugation with Ficoll (Pharmacy, LUMC, the Netherlands) and subsequently using magnetic-activated cell sorting with anti-CD14-coated microbeads (Miltenyi Biotec, Auburn, CA, USA). Purified CD14+ monocytes were cultured for 6 days at 37°C/5% CO₂ using Gibco Dutch modified Roswell Park Memorial Institute (RPMI) 1640 medium (ThermoFisher Scientific, Landsmeer, the Netherlands), which was supplemented with 10% fetal calf serum (FCS), 2 mM L-glutamine (PAA, Linz, Austria), 100 units/mL penicillin, 100 µg/mL streptomycin, and either 5 ng/mL granulocyte-macrophage colony-stimulating factor (GM-CSF, ThermoFisher Scientific) for pro-inflammatory M1 macrophage differentiation or 50 ng/mL macrophage colony-stimulating factor (M-CSF, R&D Systems, Abingdon, UK)

for anti-inflammatory M2 macrophage differentiation. One day prior to experiments, macrophages were harvested and seeded into flat-bottom 96-well plates (30,000 cells/well), if not indicated otherwise, in RPMI+10% FCS + 2 mM L-glutamine (without antibiotics or cytokines). Macrophage differentiation was quality controlled by quantifying cell surface marker expression (CD11b, CD1a, CD14, and CD163) using flow cytometry and secretion of cytokines (IL-10 and IL-12) following a 24-hour stimulation with 100 ng/mL lipopolysaccharide (InvivoGen, San Diego, USA).

4.3 Bacterial cultures

The Mav laboratory strain 101 (700898, ATCC, VA, USA) was transformed to express Wasabi, as previously described (31). Both Mav and Mav-Wasabi strains were cultured in Difco Middlebrook 7H9 broth, supplemented with 10% ADC (albumin, dextrose, and catalase) enrichment, (both from Becton Dickinson, Breda, the Netherlands), 0.2% glycerol (Merck Life Science, Amsterdam, the Netherlands), 0.05% Tween-80 (Merck Life Science), and in case of Mav-Wasabi, also with 100 μ g/ml of Hygromycin B (Life Technologies). Bacteria were diluted twice weekly based on optical density at 600 nm (OD $_{600}$) measurements. Prior to experiments, bacterial concentrations were determined by measuring the OD $_{600}$. The Wasabi-expressing Mav strain was used for all experiments, except for the ROS production assays.

4.4 Cell-free bacterial growth assay

To determine any effect of compounds on bacterial growth, Mav cultures were diluted to OD_{600} =0.1. These cultures were mixed 1:1 with chemical compounds or DMSO control at indicated concentrations and subsequently incubated at 37°C/5% CO_2 . Bacterial growth was monitored every other day, up to day 10 of incubation using OD_{600} measurements (Envision Multimode Plate Reader, Perkin Elmer).

4.5 Bacterial infection and treatment of cells

One day before infection, Mav culture was diluted to OD_{600} =0.25, corresponding to early log-phase growth. On the day of macrophage infection, bacteria were diluted in antibiotic-free cell culture medium to achieve a multiplicity of infection (MOI) of 10. The accuracy of the MOI was verified using a standard CFU assay (31). After adding bacteria to the cells, plates were centrifuged shortly (3 minutes at 130 rcf). After 1 hour of infection at 37°C/5% CO,, the supernatant was removed, and cells were washed with RPMI 1640 medium containing 30 µg/mL gentamicin to inactivate the remaining extracellular bacteria. Cells were then treated with compounds at the indicated concentration or an equal volume of vehicle control (DMSO 0.1%, vol/ vol), in the presence of 5 µg/mL gentamicin and incubated at 37°C/5% CO₂ until the experimental readout. After treatment, the supernatant was either harvested for lactate dehydrogenase (LDH) assay or discarded, and cells were lysed using either 100 or 125 µL of lysis buffer (H2O + 0.05% sodium dodecyl sulfate (SDS)) to assess the intracellular bacterial burden using a CFU assay or the MGIT system (31) respectively, or they were processed for further analysis. The activity of phenothiazines on the elimination of bacteria was determined by calculating the fraction of intracellular bacteria post-treatment in comparison to the control.

4.6 Lactate dehydrogenase (LDH) release assay

Cells (30,000 cells/well) were infected and treated as described for the appropriate

experiments. Supernatants were transferred to a new plate and used to quantify LDH release by reacting with the substrate mix from the Cytotoxicity Detection kit (LDH) (Merck Life Science) for 30 minutes at RT in the dark. LDH release was quantified by measuring the absorbance (A) at 485 nm using the SpectraMax i3x (Molecular Devices, San Jose, CA, USA). For the calculation of the cell viability, LDH release by samples treated with DMSO was used as the lower limit, and release by samples treated with 2% triton X-100 was used as the upper limit: ((1-(A_{sample} - A_{min} / A_{max} - A_{min}) *100%.

4.7 Western blot analysis

After infection and treatment, cells (300,000 cells/well in 24-well plates) were lysed with EBSB buffer (10% v/v glycerol, 3% SDS, 100 mM Tris-HCl, pH 6.8, supplemented with cOmplete™ EDTA-free protease inhibitor cocktail) (Sigma-Aldrich). Protein concentrations of cell lysates were measured using the Pierce™ BCA protein assay kit (ThermoFisher Scientific), as described previously (98). Protein levels of LC3-II, p62, or LAMP1 were assessed as described previously (99). In short, cell lysates were prepared and loaded on 15-well 4%-20% Mini-PROTEAN TGX Precast Protein Gel (Bio-Rad Laboratories, Veenendaal, the Netherlands). After transferring proteins to Immun-Blot PVDF membranes (Bio-Rad), the membranes were blocked with PBS containing 5% non-fat dry milk (PBS/5% milk) (Campina, Amersfoort, the Netherlands) for 45 minutes and incubated with primary antibodies for 90 minutes at RT. After two washing steps with PBS containing 0.75% Tween-20 (PBST), the membranes were incubated with secondary antibodies for 45 minutes at RT. Finally, the membranes underwent two washes with PBST before revelation using the enhanced chemiluminescence SuperSignal West Dura extended duration substrate (ThermoFisher Scientific). Protein bands were analyzed and quantified using ImageJ/ Fiji software (NIH, Bethesda, MD, USA) and normalized against actin levels

4.8 Confocal microscopy

For confocal microscopy, poly-d-lysine-coated glass-bottom 96-well plates (no. 1.5, MatTek Corporation, Ashland, MA, USA) were washed using cell culture medium, after which macrophages (30,000 cells/well) were seeded one day prior to experiments. Following infection and treatment, cells were stained for TFEB as described before (99). In short, cells were fixed using 1% (wt/vol) formaldehyde for 1 hour, permeabilized using 0.1% Triton X-100 for 10 minutes, blocked with 5% human serum diluted in PBS (PBS/5% HS) for 45 minutes, and subsequently stained with primary antibodies for 30 minutes at RT. After two washing steps with PBS/5% HS, cells were incubated with secondary antibodies for 30 minutes at RT in the dark. Finally, cells were stained with Hoechst 33342 for 10 minutes at RT in the dark. Samples were cured overnight using ProLong Glass Antifade Mountant (Invitrogen, ThermoFisher Scientific). Each well was imaged with three images using a Leica SP8WLL Confocal microscope (Leica, Amsterdam, the Netherlands) equipped with a 63× oil immersion objective. CellProfiler 3.0.0. was used for the assessment of the integrated/mean intensity of TFEB per single nucleus, followed by the calculation of the median of the images per condition to determine the nuclear presence of TFEB.

4.9 Phospholipidosis induction assay

For the assessment of phospholipidosis induction, cells (30,000 cells/well) were cultured in black 96-well plates. Following infection, cells were treated with

compounds and 5 μ M of the fluorescent phospholipid probe NBD-PE. Afterwards, cells were washed once with PBS and fluorescence was measured on the Envision Multimode Plate Reader.

4.10 ROS production assay

Cells (30,000 cells/well) were cultured in 96-well plates. Following infection, cells were treated for four hours until readout. Prior to readout, cells were incubated with 3 μM of CellROX or 5 μM MitoSOX probes for 30 minutes at 37°C/5% CO $_2$. Next, cells were washed thrice with PBS, trypsinized with 0.05% trypsin-EDTA, and scraped for collection. Fluorescence intensity was assessed by fixating samples with 1% paraformaldehyde before measuring samples at wavelength 533/30 nm (CellROX) or 585/40 nm (MitoSOX) on the BD Accuri C6 Plus flow cytometer (BD Biosciences). Fluorescence intensity was corrected for autofluorescence of cells. The analysis was performed using FlowJo v10 Software (BD Biosciences).

4.11 Statistics

For normally distributed paired datasets of more than two groups and one independent variable, repeated measures one-way ANOVA was used, and for multiple variables two-way ANOVA was used. In non-normally distributed paired data of more than two groups, the Friedman test was used to evaluate the statistical relevance of observed differences. Statistical differences were considered significant if p-values were < 0.05. Data analyses and graphical representation were performed using GraphPad Prism 9.0 (GraphPad Software, San Diego, CA, USA).

Data availability statement

Data will be made available on request.

Ethics statement

The studies involving humans were approved by Institutional Review Board of the Leiden University Medical Center, the Netherlands. The studies were conducted in accordance with the local legislation and institutional requirements. The participants provided their written informed consent to participate in this study.

Author Contributions

GK: Writing original draft, Writing review-editing, Conceptualization, Investigation, Methodology, Formal analysis, Validation, Visualization.

THMO: Writing review-editing, Conceptualization, Supervision, Project administration, Funding acquisition.

AS: Writing review-editing, Conceptualization, Methodology, Supervision, Project administration, Funding acquisition, Visualization.

Funding

This project has received funding from the Innovative Medicines Initiative 2 Joint Undertaking (IMI2 JU) (www.imi.europa.eu) under the RespiriNTM (grant N° 853932) project within the IMI AntiMicrobial Resistance (AMR) Accelerator program. The JU receives support from the European Union's Horizon 2020 research and innovation programme and EFPIA. The funders had no role in study design, data collection and analysis, decision to publish, or preparation of the manuscript. All claims expressed

in this article reflect solely the authors' view and do not necessarily represent those of the JU. The JU is not responsible for any use that may be made of the information it contains.

Acknowledgments

The authors would like to thank Kees L. M. C. Franken for the construction of the pSMT3 construct and Kimberley V. Walburg for performing the electroporation for generating the Wasabi-expressing *Mav* strain.

Conflict of Interest

The authors declare that they have no known competing financial interests or personal relationships that could have appeared to influence the work reported in this paper.

Declaration of generative AI and AI-assisted technologies in the writing process

During the preparation of this work, the author(s) used ChatGPT v4 (OpenAI, 2024) to improve the language and readability of the manuscript. After using this tool/service, the author(s) reviewed and edited the content as needed and take(s) full responsibility for the content of the publication.

References

- 1. Adjemian J, Olivier KN, Seitz AE, Holland SM, Prevots DR. Prevalence of nontuberculous mycobacterial lung disease in U.S. Medicare beneficiaries. Am J Respir Crit Care Med. 2012;185(8):881-6.
- 2. Brode S, Daley C, Marras T. The epidemiologic relationship between tuberculosis and non-tuberculous mycobacterial disease: a systematic review. The International journal of tuberculosis and lung disease. 2014;18(11):1370-7.
- 3. Marras TK, Chedore P, Ying AM, Jamieson F. Isolation prevalence of pulmonary non-tuberculous mycobacteria in Ontario, 1997 2003. Thorax. 2007;62(8):661-6.
- 4. Ringshausen FC, Wagner D, de Roux A, Diel R, Hohmann D, Hickstein L, et al. Prevalence of Nontuberculous Mycobacterial Pulmonary Disease, Germany, 2009-2014. Emerg Infect Dis. 2016;22(6):1102-5.
- 5. Griffith DE, Aksamit T, Brown-Elliott BA, Catanzaro A, Daley C, Gordin F, et al. An official ATS/IDSA statement: Diagnosis, treatment, and prevention of nontuberculous mycobacterial diseases. Am J Resp Crit Care. 2007;175(4):367-416.
- 6. Ingen Jv, Wagner D, Gallagher J, Morimoto K, Lange C, Haworth CS, et al. Poor adherence to management guidelines in nontuberculous mycobacterial pulmonary diseases. Eur Respir J. 2017;49(2):1601855.
- 7. Prevots DR, Marras TK. Epidemiology of human pulmonary infection with nontuberculous mycobacteria: a review. Clin Chest Med. 2015;36(1):13-34.
- 8. van Ingen J, Obradovic M, Hassan M, Lesher B, Hart E, Chatterjee A, et al. Nontuberculous mycobacterial lung disease caused by Mycobacterium avium complex disease burden, unmet needs, and advances in treatment developments. Expert Rev Resp Med. 2021;15(11):1387-401.
- 9. Honda JR, Knight V, Chan ED. Pathogenesis and Risk Factors for Nontuberculous Mycobacterial Lung Disease. Clinics in Chest Medicine. 2015;36(1):1-11.
- 10. Chan ED, Iseman MD. Underlying host risk factors for nontuberculous mycobacterial lung disease. Semin Respir Crit Care Med. 2013;34(1):110-23.
- 11. Huang JH, Kao PN, Adi V, Ruoss SJ. Mycobacterium avium-intracellulare Pulmonary Infection in HIV-Negative Patients Without Preexisting Lung Disease: Diagnostic and Management Limitations. Chest. 1999;115(4):1033-40.
- 12. Daley CL, Iaccarino JM, Lange C, Cambau E, Wallace RJ, Jr., Andrejak C, et al. Treatment of nontuberculous mycobacterial pulmonary disease: an official ATS/ERS/ESCMID/IDSA clinical practice guideline. Eur Respir J. 2020;56(1).
- 13. Xu HB, Jiang RH, Li L. Treatment outcomes for Mycobacterium avium complex: a systematic review and meta-analysis. Eur J Clin Microbiol. 2014;33(3):347-58.
- 14. Kwon YS, Koh WJ, Daley CL. Treatment of Mycobacterium avium Complex Pulmonary Disease. Tuberc Respir Dis (Seoul). 2019;82(1):15-26.
- 15. Kumar K, Daley CL, Griffith DE, Loebinger MR. Management of Mycobacterium avium complex and

Mycobacterium abscessus pulmonary disease: therapeutic advances and emerging treatments. Eur Respir Rev. 2022;31(163).

- 16. Saxena S, Spaink HP, Forn-Cuní G. Drug Resistance in Nontuberculous Mycobacteria: Mechanisms and Models. Biology. 2021;10(2):96.
- 17. Koh W-J. Nontuberculous Mycobacteria—Overview. Microbiology Spectrum. 2017;5(1):10.1128/microbiolspec.tnmi7-0024-2016.
- 18. Shamaei M, Mirsaeidi M. Nontuberculous Mycobacteria, Macrophages, and Host Innate Immune Response. Infect Immun. 2021;89(8):e0081220.
- 19. Lee H-J, Woo Y, Hahn T-W, Jung YM, Jung Y-J. Formation and Maturation of the Phagosome: A Key Mechanism in Innate Immunity against Intracellular Bacterial Infection. Microorganisms. 2020;8(9):1298.
- 20. Uribe-Querol E, Rosales C. Control of Phagocytosis by Microbial Pathogens. Front Immunol. 2017;8:1368.
- 21. Lv J, He X, Wang H, Wang Z, Kelly GT, Wang X, et al. TLR4-NOX2 axis regulates the phagocytosis and killing of Mycobacterium tuberculosis by macrophages. Bmc Pulm Med. 2017;17(1):194.
- 22. Li P, Chang M. Roles of PRR-Mediated Signaling Pathways in the Regulation of Oxidative Stress and Inflammatory Diseases. Int J Mol Sci. 2021;22(14).
- 23. Danelishvili L, Chinison JJJ, Pham T, Gupta R, Bermudez LE. The Voltage-Dependent Anion Channels (VDAC) of Mycobacterium avium phagosome are associated with bacterial survival and lipid export in macrophages. Scientific Reports. 2017;7(1):7007.
- 24. Danelishvili L, Bermudez LE. Mycobacterium avium MAV_2941 mimics phosphoinositol-3-kinase to interfere with macrophage phagosome maturation. Microbes Infect. 2015;17(9):628-37.
- 25. Ottenhoff TH, Verreck FA, Lichtenauer-Kaligis EG, Hoeve MA, Sanal O, van Dissel JT. Genetics, cytokines and human infectious disease: lessons from weakly pathogenic mycobacteria and salmonellae. Nat Genet. 2002;32(1):97-105.
- 26. Fatima S, Bhaskar A, Dwivedi VP. Repurposing Immunomodulatory Drugs to Combat Tuberculosis. Front Immunol. 2021;12:645485.
- 27. Czyz DM, Potluri LP, Jain-Gupta N, Riley SP, Martinez JJ, Steck TL, et al. Host-directed antimicrobial drugs with broad-spectrum efficacy against intracellular bacterial pathogens. mBio. 2014;5(4):e01534-14.
- 28. Boland R, Heemskerk MT, Forn-Cuni G, Korbee CJ, Walburg KV, Esselink JJ, et al. Repurposing Tamoxifen as Potential Host-Directed Therapeutic for Tuberculosis. mBio. 2023;14(1):e0302422.
- 29. Heemskerk MT, Korbee CJ, Esselink JJ, Dos Santos CC, van Veen S, Gordijn IF, et al. Repurposing diphenylbutylpiperidine-class antipsychotic drugs for host-directed therapy of Mycobacterium tuberculosis and Salmonella enterica infections. Sci Rep. 2021;11(1):19634.
- 30. Korbee CJ, Heemskerk MT, Kocev D, van Strijen E, Rabiee O, Franken K, et al. Combined chemical genetics and data-driven bioinformatics approach identifies receptor tyrosine kinase inhibitors as host-directed antimicrobials. Nat Commun. 2018;9(1):358.
- 31. Kilinc G, Walburg KV, Franken K, Valkenburg ML, Aubry A, Haks MC, et al. Development of Human Cell-Based In Vitro Infection Models to Determine the Intracellular Survival of Mycobacterium avium. Front Cell Infect Microbiol. 2022;12:872361.
- 32. Ploemen J-PHTM, Kelder J, Hafmans T, van de Sandt H, van Burgsteden JA, Salemink PJM, et al. Use of physicochemical calculation of pKa and CLogP to predict phospholipidosis-inducing potential: A case study with structurally related piperazines. Experimental and Toxicologic Pathology. 2004;55(5):347-55.
- 33. Jaszczyszyn A, Gasiorowski K, Swiatek P, Malinka W, Cieslik-Boczula K, Petrus J, et al. Chemical structure of phenothiazines and their biological activity. Pharmacol Rep. 2012;64(1):16-23.
- 34. Marques LO, Lima MS, Soares BG. Trifluoperazine for schizophrenia. Cochrane Database Syst Rev. 2004;2004(1):CD003545.
- 35. Channer B, Matt SM, Nickoloff-Bybel EA, Pappa V, Agarwal Y, Wickman J, et al. Dopamine, Immunity, and Disease. Pharmacol Rev. 2023;75(1):62-158.
- 36. Kilinc G, Boland R, Heemskerk MT, Spaink HP, Haks MC, van der Vaart M, et al. Host-directed therapy with amiodarone in preclinical models restricts mycobacterial infection and enhances autophagy. Microbiol Spectr. 2024;12(8):e0016724.
- 37. Liu WJ, Ye L, Huang WF, Guo LJ, Xu ZG, Wu HL, et al. p62 links the autophagy pathway and the ubiqutin-proteasome system upon ubiquitinated protein degradation. Cell Mol Biol Lett. 2016;21:29.
- 38. Sharma V, Verma S, Seranova E, Sarkar S, Kumar D. Selective Autophagy and Xenophagy in Infection and Disease. Front Cell Dev Biol. 2018;6:147.
- 39. Huang C, Lan W, Fraunhoffer N, Meilerman A, Iovanna J, Santofimia-Castano P. Dissecting the Anticancer Mechanism of Trifluoperazine on Pancreatic Ductal Adenocarcinoma. Cancers (Basel). 2019;11(12).
- 40. Xia Y, Jia C, Xue Q, Jiang J, Xie Y, Wang R, et al. Antipsychotic Drug Trifluoperazine Suppresses Colorectal Cancer by Inducing G0/G1 Arrest and Apoptosis. Front Pharmacol. 2019;10:1029.

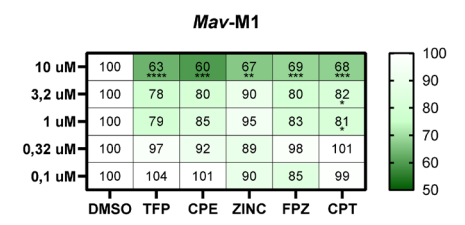
- 41. Herb M, Schramm M. Functions of ROS in Macrophages and Antimicrobial Immunity. Antioxidants (Basel). 2021:10(2).
- 42. Charbonneau ME, Passalacqua KD, Hagen SE, Showalter HD, Wobus CE, O'Riordan MXD. Perturbation of ubiquitin homeostasis promotes macrophage oxidative defenses. Sci Rep. 2019;9(1):10245.
- 43. Aruoma OI, Halliwell B, Hoey BM, Butler J. The antioxidant action of N-acetylcysteine: its reaction with hydrogen peroxide, hydroxyl radical, superoxide, and hypochlorous acid. Free Radic Biol Med. 1989;6(6):593-7.
- 44. Murphy MP, Bayir H, Belousov V, Chang CJ, Davies KJA, Davies MJ, et al. Guidelines for measuring reactive oxygen species and oxidative damage in cells and in vivo. Nat Metab. 2022;4(6):651-62.
- 45. Pedre B, Barayeu U, Ezerina D, Dick TP. The mechanism of action of N-acetylcysteine (NAC): The emerging role of H(2)S and sulfane sulfur species. Pharmacol Ther. 2021;228:107916.
- 46. Tumurkhuu G, Koide N, Dagvadorj J, Hassan F, Islam S, Naiki Y, et al. MnTBAP, a synthetic metalloporphyrin, inhibits production of tumor necrosis factor-alpha in lipopolysaccharide-stimulated RAW 264.7 macrophages cells via inhibiting oxidative stress-mediating p38 and SAPK/JNK signaling. FEMS Immunol Med Microbiol. 2007;49(2):304-11.
- 47. Reis J, Massari M, Marchese S, Ceccon M, Aalbers FS, Corana F, et al. A closer look into NADPH oxidase inhibitors: Validation and insight into their mechanism of action. Redox Biology. 2020;32:101466.
- 48. Wingler K, Altenhoefer SA, Kleikers PW, Radermacher KA, Kleinschnitz C, Schmidt HH. VAS2870 is a pan-NADPH oxidase inhibitor. Cell Mol Life Sci. 2012;69(18):3159-60.
- 49. Barrientos A, Moraes CT. Titrating the effects of mitochondrial complex I impairment in the cell physiology. J Biol Chem. 1999;274(23):16188-97.
- 50. Votyakova TV, Reynolds IJ. DeltaPsi(m)-Dependent and -independent production of reactive oxygen species by rat brain mitochondria. J Neurochem. 2001;79(2):266-77.
- 51. Hendricks O, Butterworth TS, Kristiansen JE. The in-vitro antimicrobial effect of non-antibiotics and putative inhibitors of efflux pumps on Pseudomonas aeruginosa and Staphylococcus aureus. International Journal of Antimicrobial Agents. 2003;22(3):262-4.
- 52. Nehme H, Saulnier P, Ramadan AA, Cassisa V, Guillet C, Eveillard M, et al. Antibacterial activity of antipsychotic agents, their association with lipid nanocapsules and its impact on the properties of the nanocarriers and on antibacterial activity. PLoS One. 2018;13(1):e0189950.
- 53. Bettencourt MV, Bosne-David S, Amaral L. Comparative in vitro activity of phenothiazines against multidrug-resistant Mycobacterium tuberculosis. International Journal of Antimicrobial Agents. 2000;16(1):69-71.
- 54. Kristiansen JE, Vergmann B. THE ANTIBACTERIAL EFFECT OF SELECTED PHENOTHIAZINES AND THIOXANTHENES ON SLOW-GROWING MYCOBACTERIA. Acta Pathologica Microbiologica Scandinavica Series B: Microbiology. 1986;94B(1-6):393-8.
- 55. Advani MJ, Siddiqui I, Sharma P, Reddy H. Activity of trifluoperazine against replicating, non-replicating and drug resistant M. tuberculosis. PLoS One. 2012;7(8):e44245.
- 56. Amaral L, Kristiansen JE, Abebe LS, Millett W. Inhibition of the respiration of multi-drug resistant clinical isolates of Mycobacterium tuberculosis by thioridazine: potential use for initial therapy of freshly diagnosed tuberculosis. J Antimicrob Chemother. 1996;38(6):1049-53.
- 57. Gadre DV, Talwar V. In vitro susceptibility testing of Mycobacterium tuberculosis strains to trifluoperazine. J Chemother. 1999;11(3):203-6.
- 58. Gadre DV, Talwar V, Gupta HC, Murthy PS. Effect of trifluoperazine, a potential drug for tuberculosis with psychotic disorders, on the growth of clinical isolates of drug resistant Mycobacterium tuberculosis. Int Clin Psychopharmacol. 1998;13(3):129-31.
- 59. Ratnakar P, Murthy PS. Trifluoperazine inhibits the incorporation of labelled precursors into lipids, proteins and DNA of Mycobacterium tuberculosis H37Rv. FEMS Microbiol Lett. 1993;110(3):291-4.
- 60. Deshpande D, Srivastava S, Musuka S, Gumbo T. Thioridazine as Chemotherapy for Mycobacterium avium Complex Diseases. Antimicrob Agents Chemother. 2016;60(8):4652-8.
- 61. Ordway D, Viveiros M, Leandro C, Bettencourt R, Almeida J, Martins M, et al. Clinical concentrations of thioridazine kill intracellular multidrug-resistant Mycobacterium tuberculosis. Antimicrob Agents Chemother. 2003;47(3):917-22.
- 62. Andersson Jourdan A, Peniche Alex G, Galindo Cristi L, Boonma P, Sha J, Luna Ruth A, et al. New Host-Directed Therapeutics for the Treatment of Clostridioides difficile Infection. mBio. 2020;11(2):10.1128/mbio.00053-20.
- 63. Andersson Jourdan A, Fitts Eric C, Kirtley Michelle L, Ponnusamy D, Peniche Alex G, Dann Sara M, et al. New Role for FDA-Approved Drugs in Combating Antibiotic-Resistant Bacteria. Antimicrobial Agents and Chemotherapy. 2016;60(6):3717-29.
- 64. Andersson JA, Sha J, Kirtley ML, Reyes E, Fitts EC, Dann SM, et al. Combating Multidrug-Resistant

- Pathogens with Host-Directed Nonantibiotic Therapeutics. Antimicrob Agents Chemother. 2018;62(1).
- 65. Silva T, Moreira AC, Nazmi K, Moniz T, Vale N, Rangel M, et al. Lactoferricin Peptides Increase Macrophages' Capacity To Kill Mycobacterium avium. mSphere. 2017;2(4).
- 66. Crowle AJ, Dahl R, Ross E, May MH. Evidence that vesicles containing living, virulent Mycobacterium tuberculosis or Mycobacterium avium in cultured human macrophages are not acidic. Infect Immun. 1991;59(5):1823-31.
- 67. Frehel C, de Chastellier C, Lang T, Rastogi N. Evidence for inhibition of fusion of lysosomal and prelysosomal compartments with phagosomes in macrophages infected with pathogenic Mycobacterium avium. Infect Immun. 1986;52(1):252-62.
- 68. Li A, Chen X, Jing Z, Chen J. Trifluoperazine induces cellular apoptosis by inhibiting autophagy and targeting NUPR1 in multiple myeloma. FEBS Open Bio. 2020;10(10):2097-106.
- 69. Prozialeck WC, Weiss B. Inhibition of calmodulin by phenothiazines and related drugs: structure-activity relationships. Journal of Pharmacology and Experimental Therapeutics. 1982;222(3):509.
- 70. Berchtold MW, Villalobo A. The many faces of calmodulin in cell proliferation, programmed cell death, autophagy, and cancer. Biochim Biophys Acta. 2014;1843(2):398-435.
- 71. Otreba M, Stojko J, Rzepecka-Stojko A. The role of phenothiazine derivatives in autophagy regulation: A systematic review. J Appl Toxicol. 2023;43(4):474-89.
- 72. Kusner DJ. Mechanisms of mycobacterial persistence in tuberculosis. Clinical Immunology. 2005;114(3):239-47.
- 73. Malik ZA, Iyer SS, Kusner DJ. Mycobacterium tuberculosis Phagosomes Exhibit Altered Calmodulin-Dependent Signal Transduction: Contribution to Inhibition of Phagosome-Lysosome Fusion and Intracellular Survival in Human Macrophages1. The Journal of Immunology. 2001;166(5):3392-401.
- 74. Zhang Y, Nguyen DT, Olzomer EM, Poon GP, Cole NJ, Puvanendran A, et al. Rescue of Pink1 Deficiency by Stress-Dependent Activation of Autophagy. Cell Chem Biol. 2017;24(4):471-80 e4.
- 75. Martins M, Viveiros M, Amaral L. Inhibitors of Ca2+ and K+ transport enhance intracellular killing of M. tuberculosis by non-killing macrophages. In Vivo. 2008;22(1):69-75.
- 76. Conway KL, Kuballa P, Song JH, Patel KK, Castoreno AB, Yilmaz OH, et al. Atg16l1 is required for autophagy in intestinal epithelial cells and protection of mice from Salmonella infection. Gastroenterology. 2013;145(6):1347-57.
- 77. Zhang Y, Nguyen DT, Olzomer EM, Poon GP, Cole NJ, Puvanendran A, et al. Rescue of Pink1 Deficiency by Stress-Dependent Activation of Autophagy. Cell Chemical Biology. 2017;24(4):471-80.e4.
- 78. Canton M, Sanchez-Rodriguez R, Spera I, Venegas FC, Favia M, Viola A, et al. Reactive Oxygen Species in Macrophages: Sources and Targets. Front Immunol. 2021;12:734229.
- 79. Xia Y, Xu F, Xiong M, Yang H, Lin W, Xie Y, et al. Repurposing of antipsychotic trifluoperazine for treating brain metastasis, lung metastasis and bone metastasis of melanoma by disrupting autophagy flux. Pharmacol Res. 2021;163:105295.
- 80. West AP, Brodsky IE, Rahner C, Woo DK, Erdjument-Bromage H, Tempst P, et al. TLR signalling augments macrophage bactericidal activity through mitochondrial ROS. Nature. 2011;472(7344):476-80.
- 81. Rost LM, Louet C, Bruheim P, Flo TH, Gidon A. Pyruvate Supports RET-Dependent Mitochondrial ROS Production to Control Mycobacterium avium Infection in Human Primary Macrophages. Front Immunol. 2022;13:891475.
- 82. Snyder SH, Banerjee SP, Yamamura HI, Greenberg D. Drugs, neurotransmitters, and schizophrenia. Science. 1974;184(4143):1243-53.
- 83. Stone JM, Morrison PD, Pilowsky LS. Glutamate and dopamine dysregulation in schizophrenia--a synthesis and selective review. J Psychopharmacol. 2007;21(4):440-52.
- 84. Nolan RA, Reeb KL, Rong Y, Matt SM, Johnson HS, Runner K, et al. Dopamine activates NF-κB and primes the NLRP3 inflammasome in primary human macrophages. Brain, Behavior, & Immunity Health. 2020;2:100030.
- 85. Gaskill PJ, Carvallo L, Eugenin EA, Berman JW. Characterization and function of the human macrophage dopaminergic system: implications for CNS disease and drug abuse. J Neuroinflammation. 2012;9:203.
- 86. Nolan RA, Muir R, Runner K, Haddad EK, Gaskill PJ. Role of Macrophage Dopamine Receptors in Mediating Cytokine Production: Implications for Neuroinflammation in the Context of HIV-Associated Neurocognitive Disorders. J Neuroimmune Pharmacol. 2019;14(1):134-56.
- 87. Cooper AM, Mayer-Barber KD, Sher A. Role of innate cytokines in mycobacterial infection. Mucosal Immunology. 2011;4(3):252-60.
- 88. Sasindran SJ, Torrelles JB. Mycobacterium Tuberculosis Infection and Inflammation: what is Beneficial for the Host and for the Bacterium? Frontiers in Microbiology. 2011;2.
- 89. Park HE, Lee W, Choi S, Jung M, Shin MK, Shin SJ. Modulating macrophage function to reinforce

host innate resistance against Mycobacterium avium complex infection. Front Immunol. 2022;13:931876.

- 90. Lahti RA, Evans DL, Stratman NC, Figur LM. Dopamine D4 versus D2 receptor selectivity of dopamine receptor antagonists: possible therapeutic implications. European Journal of Pharmacology. 1993;236(3):483-6.
- 91. Salie S, Hsu N-J, Semenya D, Jardine A, Jacobs M. Novel non-neuroleptic phenothiazines inhibit Mycobacterium tuberculosis replication. J Antimicrob Chemoth. 2014;69(6):1551-8.
- 92. Midha KK, Korchinski ED, Verbeeck RK, Roscoe RM, Hawes EM, Cooper JK, et al. Kinetics of oral trifluoperazine disposition in man. Br J Clin Pharmacol. 1983;15(3):380-2.
- 93. Vibe CB, Fenaroli F, Pires D, Wilson SR, Bogoeva V, Kalluru R, et al. Thioridazine in PLGA nanoparticles reduces toxicity and improves rifampicin therapy against mycobacterial infection in zebrafish. Nanotoxicology. 2016;10(6):680-8.
- 94. Abukhalid N, Islam S, Ndzeidze R, Bermudez LE. Mycobacterium avium Subsp. hominissuis Interactions with Macrophage Killing Mechanisms. Pathogens. 2021;10(11).
- 95. Braunstein M, Espinosa BJ, Chan J, Belisle JT, Jacobs WR, Jr. SecA2 functions in the secretion of superoxide dismutase A and in the virulence of Mycobacterium tuberculosis. Mol Microbiol. 2003;48(2):453-64.
- 96. Ng VH, Cox JS, Sousa AO, MacMicking JD, McKinney JD. Role of KatG catalase-peroxidase in mycobacterial pathogenesis: countering the phagocyte oxidative burst. Mol Microbiol. 2004;52(5):1291-302.
- 97. Sherman DR, Sabo PJ, Hickey MJ, Arain TM, Mahairas GG, Yuan Y, et al. Disparate responses to oxidative stress in saprophytic and pathogenic mycobacteria. Proc Natl Acad Sci U S A. 1995;92(14):6625-9.
- 98. van Doorn CLR, Schouten GK, van Veen S, Walburg KV, Esselink JJ, Heemskerk MT, et al. Pyruvate Dehydrogenase Kinase Inhibitor Dichloroacetate Improves Host Control of Salmonella enterica Serovar Typhimurium Infection in Human Macrophages. Front Immunol. 2021;12:739938.
- 99. Kilinc G, Boland R, Heemskerk MT, Spaink HP, Haks MC, van der Vaart M, et al. Host-directed therapy with amiodarone in preclinical models restricts mycobacterial infection and enhances autophagy. Microbiol Spectr. 2024:e0016724.

Supplementary material

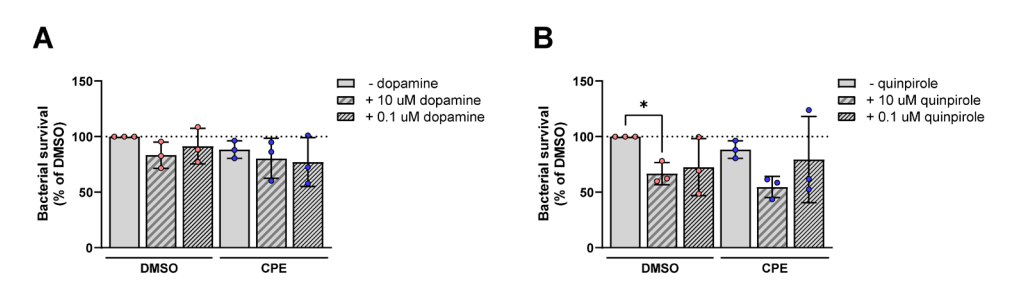


Supplementary Figure 1. Identification of phenothiazines as host-directed therapeutics against *Mav* in primary human macrophages.

Bacterial survival of Mav within M1 macrophages after treatment with 10, 3.2, 1, 0.32, or 0.1 μ M of five phenothiazines or DMSO for 24 hours, as determined by the MGIT assay. Data represent the mean \pm standard deviation (SD) from minimally four donors. Dots represent the mean from triplicate wells of a single donor. Bacterial survival is expressed as a percentage of DMSO (=100%) per donor. Statistical significance was tested using a two-way ANOVA with Dunnett's multiple comparisons test. Asterisks depict the significance of treatments.

TFP; trifluoperazine, CPE; chlorproethazine, ZINC; ZINC2187528, FPZ; fluphenazine, CPT; chlorprothixene.

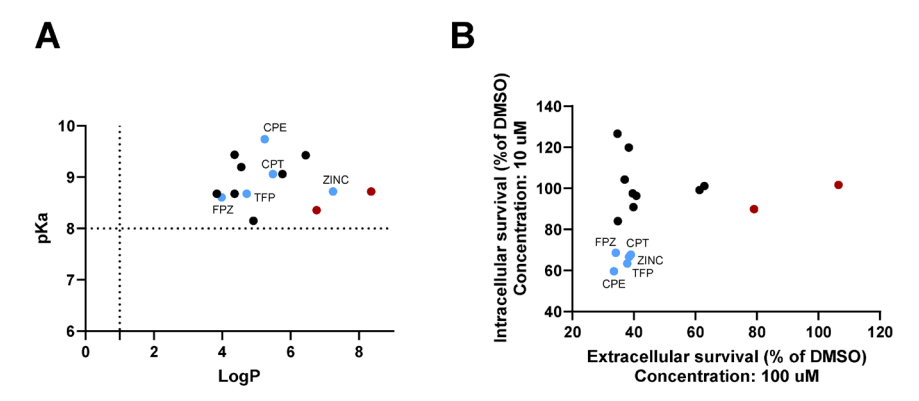
* = p<0.05, ** = p<0.01, *** = p<0.001 and **** = p<0.0001.



Supplementary Figure 2. Physical properties of 16 phenothiazines associated with intracellular drug accumulation.

(A) The 16 phenothiazines are graphed in relation to pKa (basic) and logP. The exclusion limits of the Ploemen models are delineated by the dotted lines. Blue dots represent the analogs that impaired the survival of Mav in primary human macrophages, whereas the black dots represent compounds that were not effective. (B) Bacterial survival in Mav-infected macrophages after treatment with 10 μ M of the phenothiazines or DMSO for 24 hours (Figure 1A) in comparison to bacterial survival in planktonic culture (absent of macrophages) after treatment with 100 μ M of the drugs or DMSO.

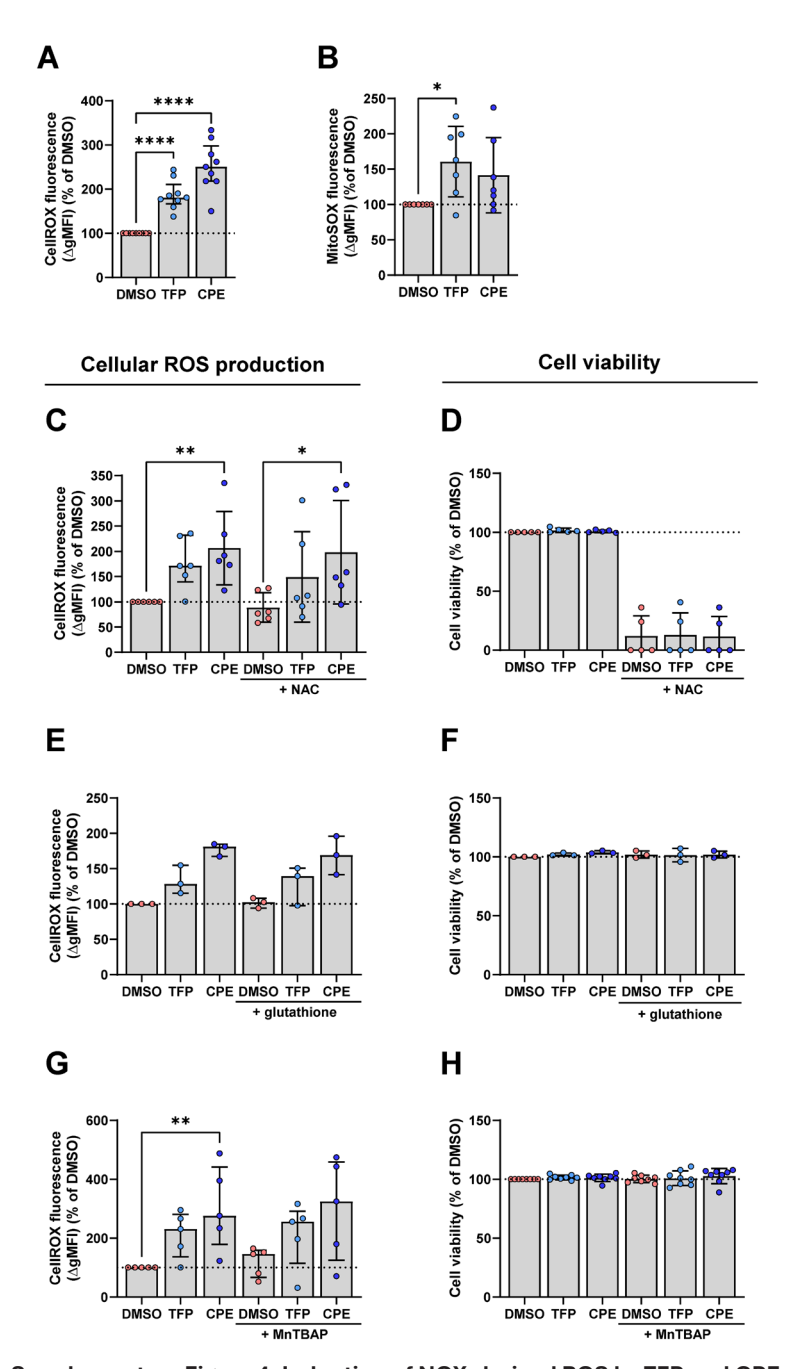
TFP; trifluoperazine, CPE; chlorproethazine, ZINC; ZINC2187528, FPZ; fluphenazine and CPT; chlorprothixene.



Supplementary Figure 3. Effect of dopamine agonists on intracellular ${\it Mav}$ control with or without phenothiazines.

(A-B) Bacterial survival of Mav within M1 macrophages, where dopamine (A) or quinpirole (B) was applied alone for the first hour, followed by the addition of 10 μ M of CPE or DMSO for the remainder of the treatment. After 24 hours of treatment, bacterial survival was determined by the CFU assay. Data represents the mean \pm SD (n=3), and dots represent the mean from duplicate wells of a single donor. Bacterial survival is expressed as a percentage of DMSO (=100%, indicated with the dotted line) per donor. Statistical significance was tested using a repeated-measures one-way ANOVA with Bonferroni's multiple comparisons test. CPE; chlorproethazine.

^{* =} p < 0.05.

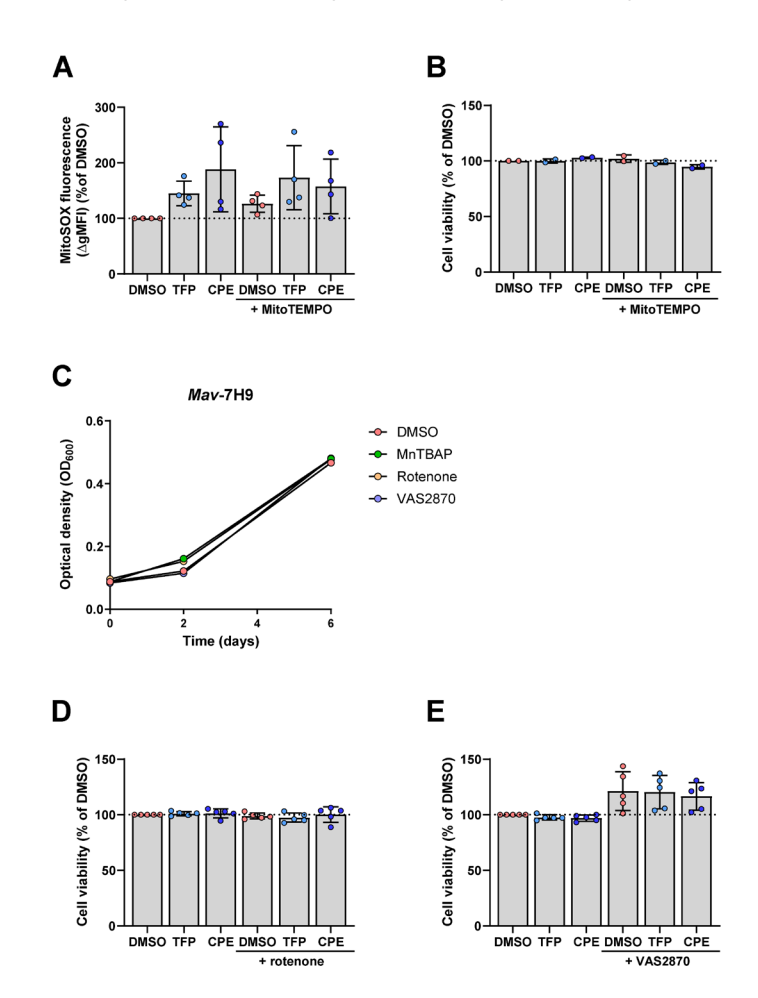


Supplementary Figure 4. Induction of NOX-derived ROS by TFP and CPE might have a limited role in their enhanced macrophage response against *Mav*.

(A-B) M1 macrophages were treated with 10 μ M TFP, CPE, or DMSO for 4 hours. Total cellular ROS production (A) or mitochondrial ROS (B) production was measured by flow cytometry. Data represent the median \pm interquartile range from 8 donors (A) or mean \pm SD from 7 donors (B). Statistical significance was tested using a Friedman test with Dunn's multiple comparisons

test (A) or a repeated-measures one-way ANOVA with Dunnett's multiple comparisons test (B). (C-D) M1 macrophages were treated for 4 (C) or 24 (D) hours with 10 µM TFP, CPE, or DMSO with or without 5 mM N-acetyl-cysteine (NAC). Total cellular ROS production was detected by flow cytometry. The geometric mean fluorescence intensity (ΔgMFI) (C) or cell viability (D) were determined. Data represent the median ± interquartile range from 6 donors (C) or mean ± SD from 5 donors (D). Statistical significance was tested using a Friedman test with Dunn's multiple comparisons test (C), (E-F) M1 macrophages were treated with 10 µM TFP, CPE, or DMSO with or without 100 µM L-glutathione for 4 (E) or 24 (F) hours. Total cellular ROS production was detected by flow cytometry. The geometric mean fluorescence intensity (ΔgMFI) (E) or cell viability (F) were determined. Data represent the median ± interquartile range from 3 donors (E) or mean ± SD from 3 donors (F). Statistical significance was tested using a Friedman test with Dunn's multiple comparisons test (E). (G-H) M1 macrophages were treated with 10 µM TFP. CPE, or DMSO with or without 100 µM MnTBAP for 4 (G) or 24 (H) hours. Total cellular ROS production was detected by flow cytometry. The geometric mean fluorescence intensity (ΔgMFI) (E) or cell viability (F) were determined. Data represent the median ± interquartile range from 5 donors (G) or mean ± SD from 5 donors (H). Statistical significance was tested using a Friedman test with Dunn's multiple comparisons test (G). Dots represent the mean from duplicate wells of a single donor. Data is expressed as a percentage of vehicle control DMSO (=100%, indicated with the dotted line) per donor.

TFP; trifluoperazine, CPE; chlorproethazine. * = p<0.05, ** = p<0.01 and **** = p<0.0001.



Supplementary Figure 5. Induction of NOX-derived ROS by TFP and CPE might have a limited role in their enhanced macrophage response against *Mav*.

(A-B) M1 macrophages were treated with 10 μ M TFP, CPE, or DMSO with or without 10 μ M MitoTEMPO for 4 (A) or 24 (B) hours after *Mav* infection. Total mitochondrial ROS production was detected by flow cytometry. The geometric mean fluorescence intensity (Δ gMFI) (A) or cell viability (B) were determined. Data represent the mean \pm SD from different donors (n=4). Statistical significance was tested using a repeated-measures one-way ANOVA with Bonferroni's multiple comparisons test (A). (C) Growth of Mav in liquid broth up to 10 days after exposure to 100 μ M MnTBAP, 5 μ M rotenone, 10 μ M VAS2870, or DMSO. Data represent the mean \pm SD of triplicate wells from two independent experiments. (D-E) Percentage of viable M1 macrophages after treatment with 5 μ M rotenone (D), 10 μ M VAS2870 (E), or DMSO 24 hours. Data represent the mean \pm SD from 5 (D). Dots represent the mean from duplicate wells of a single donor. Data is expressed as a percentage of vehicle control DMSO (=100%, indicated with the dotted line) per donor.

TFP; trifluoperazine, CPE; chlorproethazine.